Exact Analytical Solutions for Modelling the Speed-Time Characteristics of Direct-Start Induction Machines under Various Operational Conditions on Ships: Review and Experimental Validation

Ilija Knezevic[1], Martin Calasan[2], Tatijana Dlabac[1,*], Filip Filipovic[3], Nebojsa Mitrovic[3]
[1]Faculty of Maritime Studies Kotor, University of Montenegro,
Put I Bokeljske brigade 44, Dobrota, 85331 Kotor, Montenegro
[2]Faculty of Electrical Engineering, University of Montenegro,
Dzordza Vasingtona bb, 81000 Podgorica, Montenegro
[3]Faculty of Electronic Engineering, University of Nis,
Aleksandra Medvedeva 4, 18104 Nis, Serbia
*ilijak@ucg.ac.me; martinc@ucg.ac.me; *tanjav@ucg.ac.me; filip.filipovic@elfak.ni.ac.rs; nebojsa.mitrovic@elfak.ni.ac.rs*

***Abstract*—Induction machines (IMs) are crucial to driving auxiliary machinery and devices of ships, such as pumps, fans, winches, and elevators, which are essential for maintaining the operational functions of a ship and are characterised by various types of loads. This is of critical importance because high surges of starting current can cause instabilities and fluctuations in a ship's power system, directly affecting the safety and efficiency of ship operations. This paper provides a comprehensive review of analytical expressions for modelling the start-up time of directly started IMs under different ship operational conditions (no-load, linear load, fan load, and gravitational load). Validation of the analytical models was performed by comparing the speed-time characteristics obtained from the experimental measurements with the corresponding ones obtained by simulations in a MATLAB Simulink environment. The observed 1.5 kW IM reached a steady state for 0.1356 seconds when driving the load with a fan characteristic. However, when subjected to linear and gravitational loads, the IM requires longer times to reach a steady state - 0.1400 and 0.1606 seconds, respectively. The results of the simulations and experimental tests highly corresponded with the analytical predictions, confirming the reliability and practical applicability of the analytical models.**

***Index Terms*—Directly started; Induction machine; Modelling; Ship auxiliary machinery.**

I. INTRODUCTION

A. Background and Idea behind the Research

In the maritime industry, three-phase induction machines (IMs) with squirrel-cage rotors are key elements of propulsion systems due to their exceptional reliability, efficiency, and simple construction [1]. These IMs are specifically designed to withstand demanding maritime conditions, making them indispensable for various ship operations [2], [3].

Manuscript received 19 August, 2024; accepted 22 November, 2024.

On ships, consumers can be classified according to their functions into categories such as propulsion machines, auxiliary machines, deck machines and devices, hotel consumers, and general needs of the ship [4], [5]. IMs, which are often power deck machines and devices, as well as auxiliary ship machines, are characterised by specific load characteristics [6], [7]. These load characteristics of IMs can be categorised into the four most important groups [8]: fan-type loads, gravitational loads, linear loads, and hyperbolic loads.

The gravitational load characteristic implies a constant torque as a function of speed and is often found in cargo, tension, and anchor winches, compressors, hoists, and cranes. On the other hand, the fan type, often called the "propeller characteristic", is predominant in the operation of propellers, pumps, fans, and thrusters [9]. IMs on ships with linear load characteristics can be found in specific devices, such as winders [4]. The hyperbolic load characteristic is found in ship applications for drives that require constant power.

The starting of an IM is a critical phase [10], as the current can reach up to nine times the nominal value, causing significant disturbances in the power network of the ship [11]–[13]. These disturbances not only affect the stability of the network, but also create oscillations in the quality of the power supply, affecting sensitive systems such as navigation and communication [14]–[16]. Additionally, high starting currents can reduce machine lifespan, leading to higher maintenance costs [17], [18]. To mitigate these effects, appropriate techniques are required to limit the starting current [19], [20]. Various methods such as direct online starting [21], star-delta starters [22], [23], autotransformers [24], soft starters [25], and inverters are commonly used [26], each with its own advantages and limitations.

The motivation for this research arises from the need to accurately model the dynamic behaviour of IMs in shipboard

environments, especially during transient conditions like starting and load changes. These processes affect power quality and equipment lifespan. Reliable models are crucial to understanding these effects and improving the performance and reliability of shipboard electrical systems.

B. Literature Review

Modelling the operation of an IM involves solving nonlinear differential equations that adequately describe its function [27], [28]. The speed-time curve of a machine can be represented via numerical techniques in the time domain or through analytical expressions. The numerical approach, which uses integration techniques to solve a set of equations, is implemented in several software packages to simulate electrical machines. Although this method is demanding in terms of the execution time required, due to the complexity and scope of the equations that are solved, it allows precise modelling and provides detailed information on the machine's operation.

Analytical approaches to calculate IM start-up time are divided into two categories. The first includes analytical expressions to model the speed-time characteristics without load. For example, Aree [29] proposes a simplified first-order motor model for conventional starting methods, while Ćalasan [30] presents a formula derived using the Lambert W function to calculate start-up time under no-load conditions based on Kloss's torque equation. Similarly, Ćalasan [31] provides an expression based on the equivalent circuit and Thevenin's torque equation, using an iterative process with the Lambert W function for the calculation of the inverse speed-time during direct no-load starts. The second category focusses on modelling speed-time characteristics under load, crucial in maritime settings. Various dynamic models have been developed, such as those in [32], which describe started IMs directly, taking into account bearing losses. Additionally, Knežević, Ćalasan, and Dlabač [33] review ship loads, particularly fan loads, providing precise analytical expressions for speed-time characteristics using the torque equations of Kloss and Thevenin. In [34], a formula was also introduced to present speed-time characteristics under gravitational loads.

C. Contribution and Novelty

The key contributions and novelties of this paper are as follows.

– A comprehensive review and analysis of analytical methods for calculating IM start-up times under various shipboard loads, including linear, fan, and gravitational load characteristics, as well as no-load conditions.

– Simulations validating the theoretical dynamic models of speed-time characteristics, conducted under varying inertia moments and load coefficients.

– Experimental validation of theoretical expressions on a 1.5 kW IMs, confirming their practical applicability and reliability.

– A novel comparative analysis of IM performance with different shipboard loads under identical conditions has not been previously addressed in the literature. This analysis examines the speed-time characteristics of various loads both through simulations and experimental measurements.

– The analytical models presented are crucial for adjusting overcurrent protection devices and evaluating power quality in shipboard electrical systems.

D. Paper Organisation

This paper is organised into five sections. Section II provides a detailed examination of the analytical approaches for modelling the speed-time characteristics of directly started IMs under various types of loads. In Section III, simulations of different dynamic models are conducted to describe the speed-time characteristics. The experimental results are presented in Section IV. Section V provides the key findings of the study and possible directions for future research.

II. Analytical Solutions for Modelling the Speed-Time Curves of Induction Machines under Various Operating Conditions

This section presents analytical formulas for calculating the start-up time of an induction machine under various load conditions on a ship. With regard to the mechanical subsystem and shipboard loads, nearly all types of load are considered. The analytical expressions for the start-up time presented in this section are derived from the parameters of the equivalent Thevenin circuit. The relationships and parameters of the Thevenin equivalent circuit are thoroughly detailed in [33], [34].

A. No-Load Operation

In [30], an analytical formula is presented to calculate the time required to start a direct-starting IM in no-load mode. This formula was derived from the Kloss formula for torque and is given in the following form

$$t = \frac{J\omega_s}{2M_{br}}\left(\frac{1-s^2}{2s_{br}} - s_{br}\log(s)\right). \tag{1}$$

In addition to the formula mentioned above, in [31], another formula is proposed derived from the expression for torque determined from the Thevenin equivalent circuit of the IM

$$t = \frac{J\omega_s}{U_T{}^2 R_2}\left(\frac{\left(R_T{}^2 + \left(X_T + X_2\right)^2\right)}{2}\left(1-s^2\right) + 2R_T R_2\left(1-s\right) - R_2{}^2\log(s)\right). \tag{2}$$

B. Linear Load Type

In marine applications, IMs often operate under various load characteristics. In this context, the linear load characteristic is described as follows

$$M_L = B_L \times (1-s)\,\omega_s. \tag{3}$$

In the equation, M_L represents the load torque, ω_s represents the synchronous speed of the machine, B_L represents the coefficient of linear loading, and s represents the slip of the machine. An analytical solution, proposed in [32], which describes the speed-time characteristic of a IM

that is started directly under a linear load, is given as follows:

$$\begin{aligned} t &= I_1 + I_2 + I_3, \\ I_1 &= k_1 \log(1-s_1) - k_1 \log(s-s_1), \\ I_2 &= \frac{2k_3}{\sqrt{4r_3r_1 - r_2^2}} \begin{pmatrix} \frac{\tan^{-1}(2r_2 + r_2)}{\sqrt{4r_3r_1 - r_2^2}} \\ -\frac{\tan^{-1}(2r_1s + r_2)}{\sqrt{4r_3r_1 - r_2^2}} \end{pmatrix}, \\ I_3 &= k_2 \begin{pmatrix} \frac{1}{2r_1}(\log(r_1 + r_2 + r_3)) \\ -\log(r_1s^2 + r_2s + r_3) \end{pmatrix} - \frac{r_2}{2r_1}\frac{I_2}{k_3}. \end{aligned} \quad (4)$$

The entire procedure to determine all the unknown coefficients can be found in [32].

C. Fan Load Type

The most commonly encountered load characteristic of ships is the fan-type load, which can be described as follows

$$M_L = B_F \times (1-s)^2 \omega_s^2, \quad (5)$$

where M_L is the load torque, B_F is the fan load coefficient, ω_s is the synchronous speed, and s represents the slip.

In [33], the modelling of the speed-time characteristics of a IM directly started when driving a fan-type load on a ship was performed and explained in detail. The derived expression is given in the following form

$$\begin{aligned} t &= k_1 \log\left(\frac{1-s_1}{s-s_1}\right) + \\ &+ \left(k_2 - \frac{r_2}{2r_1k_4}\right)\log\left(\frac{1-s_2}{s-s_2}\right) + \\ &+ \frac{k_3}{2r_1}\log\left(\frac{r_1 + r_2 + r_3}{r_1s^2 + r_2s + r_3}\right) + \\ &+ \frac{2k_4}{4r_3r_1 - r_2^2}\begin{pmatrix} \tan^{-1}(2r_1 + r_2) \\ -\tan^{-1}(2r_1s + r_2) \end{pmatrix}. \end{aligned} \quad (6)$$

D. Gravitational Load Type

The gravitational load characteristic of a ship, where the load torque (M_L) is equal to the gravitational constant (B_G), i.e., the load torque is constant and independent of the rotational speed, can be expressed as follows

$$M_L = B_G, \quad (7)$$

In [34], modelling of the start-up time was performed for a IM directly started driving a gravitational load type. Two expressions for time were derived, both with identical mathematical formulations. The first expression was obtained by applying Kloss's torque equation, while the second was derived from the torque expression via Thevenin's equivalent circuit. The expression obtained for time as a function of slip is given in the following form

$$\begin{aligned} t &= \frac{\alpha_1}{\alpha_4}(s-1) + \frac{\alpha_1}{\alpha_4}k_1 \log\left(\frac{s-s_1}{1-s_1}\right) + \\ &+ \frac{\alpha_1}{\alpha_4}k_2 \log\left(\frac{s-s_2}{1-s_2}\right). \end{aligned} \quad (8)$$

III. Simulation Results

In this section, simulation results are presented to analyse and verify the analytical expressions for modelling the speed-time characteristics of directly started IMs. Specifically, the simulation results of the IM under no-load conditions and while driving fan-type and linear loads are shown. Additionally, a comparison of different ship loads operating at the same operating point is presented. The IM used in the simulation tests was selected from the Simulink library, and its parameters are provided in Table I. Speed variations observed in the simulation results are expected, as they are a direct consequence of the different load coefficients under which the motor was tested, with each load type causing changes in the IMs speed.

TABLE I. PARAMETERS OF THE INDUCTION MACHINE.

Parameters	Value
Stator resistance - R_1	1.405 Ω
Rotor resistance - R_2	1.395 Ω
Stator reactance - X_1	1.8344 Ω
Rotor reactance - X_2	1.8344 Ω
Nominal moment of inertia - J_n	0.0131 kgm^2
Nominal voltage - U_n	400 V
Nominal power - P_n	4 kW
Nominal frequency - f	50 Hz
Number of pole pairs - p	2

A. No-Load Operation

The simulation results for the start-up time of a directly started IM under no-load conditions are presented to evaluate the accuracy and variability of the analytical expressions. These results are important for understanding the behaviour of IM when no mechanical load is applied to the shaft. The following figures compare the analytical expressions for modelling the speed-time characteristics with MATLAB/Simulink simulations. Verification of analytical expressions for different moments of inertia J, $2J$, and $4J$ is shown in Fig. 1. A higher moment of inertia extends the start-up time of IM. The analytical expressions are shown to be very precise compared with the MATLAB/Simulink simulation under different moments of inertia, confirming their validity.

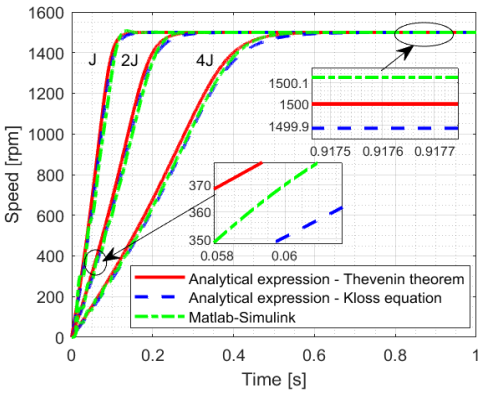

Fig. 1. Speed-time characteristics of IM under no-load conditions at $U = 200$ V.

B. *Linear Load Type*

This section presents simulation results for different operating conditions of the IM under linear load conditions. The simulation results for different moments of inertia *J*, *2J*, and *4J* are shown in Fig. 2(a). These results confirm the good agreement of the analytical expressions with the MATLAB/Simulink simulations, showing that an increase in the inertia moment prolongs the start-up time of the IM. The accuracy of analytical expressions under these conditions highlights their ability to accurately predict machine dynamics. The results of testing the analytical expressions to represent the speed-time characteristics at different linear load coefficients (0.019 and 0.19) are shown in Fig. 2(b). A higher linear load coefficient leads to a greater slip in the machine, which affects the reduced rotational speed. Under these conditions, the analytical expressions show good agreement with the MATLAB/Simulink simulations, confirming their validity and reliability under different load conditions.

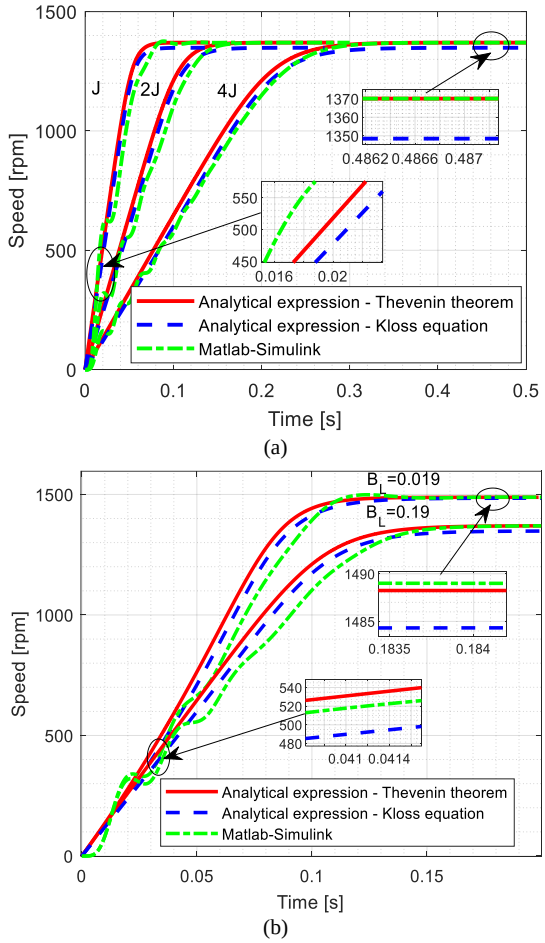

Fig. 2. Speed-time characteristics of the IM under linear loading: (a) *U = 300 V*, $B_L = 0.19$; (b) *U = 300 V*, *J = 2J*.

C. *Fan Load Type*

The simulation results for the start-up time of a directly started IM driving a fan-type load are shown in Fig. 3. As in the previous simulations, the same methodology is used to compare the analytical expressions with the MATLAB/Simulink simulations. Figure 3(a) shows the simulation and comparison for different moments of inertia. The results indicate a strong agreement of the speed-time characteristics between the analytical expressions and the MATLAB/Simulink simulations. Figure 3(b) presents the simulation results for different fan load coefficients ($B_F = 0.00015$ and $B_F = 0.0015$). A higher fan load coefficient leads to a reduction in speed. Under these conditions, the analytical expressions show very good agreement with the MATLAB/Simulink simulations, with the Thevenin model proving ideal, especially in the steady state, whereas the Kloss model tracks the results with slight deviations.

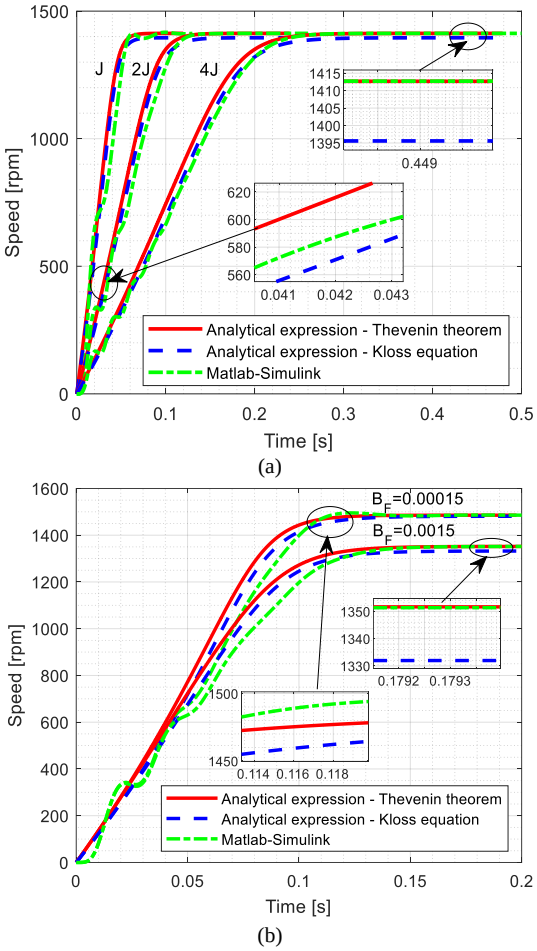

Fig. 3. Speed-time characteristics of the induction machine under fan loading: (a) *U = 300 V*, $B_L = 0.0009$; (b) *U = 300 V*, *J = 2J*.

D. *Gravitational Load Type*

The results of the verification of the analytical expressions for representing the speed-time characteristics of a directly started IM driving a gravitational load type are shown in Fig. 4.

In Fig. 4(a), where the results for different moments of inertia are presented, the MATLAB/Simulink results for the nominal moment of inertia slightly oscillate, whereas for higher inertia values these oscillations become less pronounced. The agreement of the analytical expressions with MATLAB/Simulink simulations is rather strong, confirming their accuracy under conditions of constant load torque. In Fig. 4(b), a simulation is performed for different coefficients of gravitational load. In reality, the gravitational load represents a constant torque independent of the speed. The machine started with double the moment of inertia and a voltage of *300 V*, and very good agreement between the analytical expressions and MATLAB/Simulink simulations was observed.

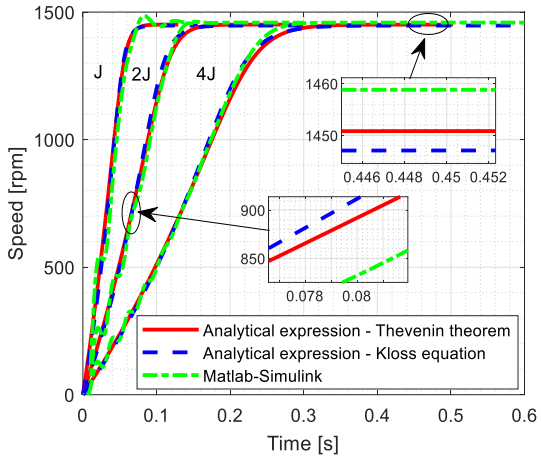

(a)

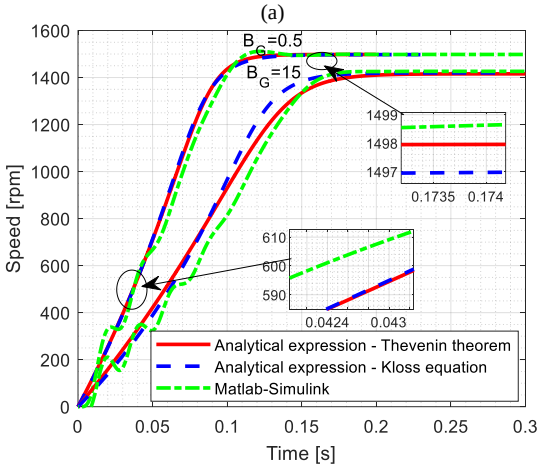

(b)

Fig. 4. Speed-time characteristics of the induction machine under gravitational loading: (a) $U = 300$ V, $J = J_n$, $B_G = 10$; (b) $U = 300$ V, $J = 2J$.

E. Performance of Shipboard Loads at the Same Operating Point

For a precise analysis of the performance of an IM under different shipboard loads, it is crucial to conduct comparisons at the same operating point, i.e., at the same load torque under steady-state conditions. Figure 5 presents a torque-speed graph illustrating the operating point at which simulations were performed to analyse the IM start-up under various shipboard loads. The simulations were carried out with a fan load coefficient $B_F = 0.00043543$, a linear load coefficient $B_L = 0.0659875$, and a gravitational load coefficient $B_G = 10$. All simulations were conducted at a voltage of 300 V and a moment of inertia $J_n = 2J$. The aim of the analysis is to compare the speed-time characteristics of the direct-start induction machine at the same operating point to determine which load allows the machine to achieve the shortest start-up time and to identify the differences in start-up time between the different types of loads. This analysis is of exceptional importance because extended start-up times, especially if they exceed the duration the machine can withstand in a short-circuit state, can become very dangerous for the machine itself. Prolonged start-up times increase thermal stress, which can lead to overheating and damage the machine's insulation.

In Fig. 5, the electromagnetic torque and the torques of different load types (fan, gravitational, and linear) are shown as functions of speed. The operating point, marked on the graph, represents the speed and torque at which the machine operates stably. Analysing the start-up at this point allows for a precise comparison of the time required to reach a steady state for each type of load.

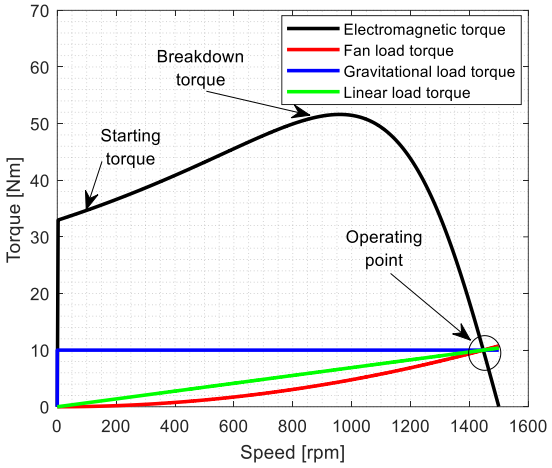

Fig. 5. Torque-speed characteristics.

Figure 6 presents the simulation results for the speed-time characteristics of a IM directly started under different shipboard loads at the same operating point.

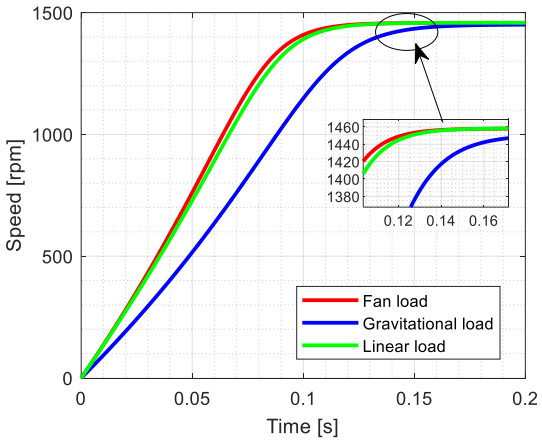

(a)

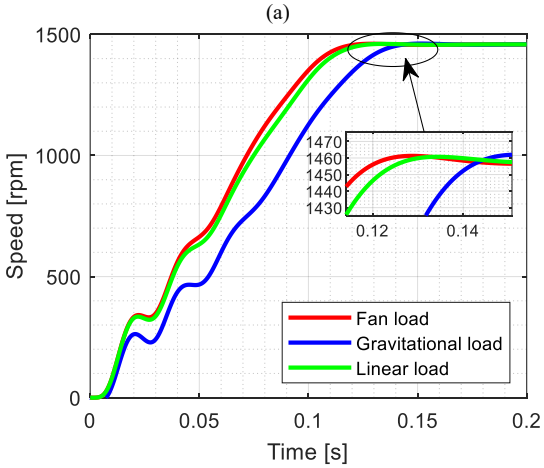

(b)

Fig. 6. Speed-time characteristics at the same operating point: (a) Results obtained through the Thevenin model; (b) Results obtained through MATLAB/Simulink simulation.

Figure 6(a) shows the simulation results obtained via the Thevenin model, and Fig. 6(b) shows the results of the MATLAB/Simulink simulations. The results of the three models are consistent, demonstrating the alignment between the analytical expressions and the MATLAB/Simulink model. The simulation results indicate that the start-up time

is the shortest for the fan load type, whereas the start-up times for the linear and gravitational load types are somewhat longer. This can be attributed to the nature of each load type and their impact on the dynamics of the IM. Owing to its quadratic relationship with speed, the type of fan load allows for faster attainment of a steady state. The linear load type, which has a torque proportional to speed, requires more time for start-up, as the load torque increases linearly with speed. The gravitational load type, with constant torque, also requires a longer start-up time because the load remains the same regardless of speed, imposing additional strain on the machine at lower speeds.

IV. EXPERIMENTAL RESULTS

The results of the experimental validation of the analytical expressions for modelling the speed-time characteristics of a directly started IM under different types of shipboard loads are presented in this section. The experimental measurements were conducted at the Laboratory for Electromotor Drives and Traction at the *Faculty of Electronic Engineering, University of Niš, Niš, Serbia*. The experimental setup is shown in Fig. 7. The IM was subjected to different types of loads to obtain speed-time characteristics, which were then compared with theoretical predictions. The measurements included no-load, fan and linear load types.

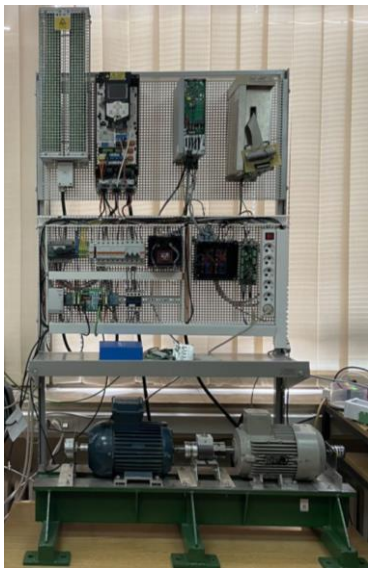

Fig. 7. Experimental setup used to measure the speed-time characteristics of the IM.

First, experiments were conducted under standard no-load and short-circuit conditions to obtain the IM parameters, which are given in Table II. The IM used for load emulation is powered by an ABB ACS 880-01 frequency converter. There are encoders on the left and right ends of the shaft. The encoder on the left end is used to measure the speed during the experiments. This encoder is programmed to output 8192 pulses per revolution. The encoder on the right end of the shaft is used by the ABB ACS 880-01 frequency converter for more precise control in the desired operating mode. This encoder outputs 1000 pulses per revolution. Pulse acquisition from the measurement encoder is performed by the dSPACE DS 1103 device every 1 ms. For the control of this device, the dedicated software *ControlDesk* is used and programming is performed in MATLAB. The speed data are stored in a MAT format suitable for processing in MATLAB. The ABB frequency converter, series ACS 880, subseries 01, is programmed to operate with direct torque control (DTC) and powers the machine. In experiments, when it is used, it powers the machine so that the machine behaves as a defined load (fan and linear). This load emulation is performed directly in the frequency converter by modifying its control algorithm through adaptive programming via *Drive composer software*. In load emulation mode, excess energy is dissipated on a braking resistor. The data of interest are recorded from the *Drive Composer software* at the highest possible resolution and stored in .csv format. This format is later converted to an MAT file for further processing. The two variables recorded are speed and load torque.

TABLE II. PARAMETERS OF THE EXPERIMENTAL IM FROM NO-LOAD AND SHORT-CIRCUIT TESTS.

Parameters	Value
Stator resistance - R_1	5.0530 Ω
Rotor resistance - R_2	3.2296 Ω
Stator reactance - X_1	5.5217 Ω
Rotor reactance - X_2	5.5217 Ω
Nominal moment of inertia - J_n	0.003487 kgm^2
Nominal voltage - U_n	400 V
Nominal power - P_n	1.5 kW
Nominal frequency - f	50 Hz
Number of pole pairs - p	1

A. No-Load Operation

Figure 8 shows the experimental results of directly starting the IM under no-load conditions without any external mechanical load applied. The aim of this experiment is to compare theoretical models based on Kloss's formula and Thevenin's theorem with experimental results to validate analytical expressions for no-load conditions. Figure 8 shows good agreement of the speed-time characteristics obtained from the analytical expressions with the experimental results. Theoretical models show high precision in predicting machine dynamics during start-up. However, since the analytical expressions represent the ideal startup of the machine and do not account for losses due to bearing friction, a slight deviation of the speed obtained experimentally from the theoretical models can be observed in the steady state.

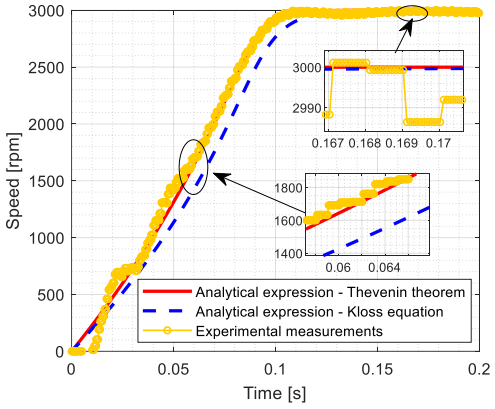

Fig. 8. Experimental results of the speed-time characteristics of the IM under no-load conditions.

B. Linear Load Type

Figure 9 shows a comparison of the speed-time characteristics obtained experimentally with the analytical expressions. IM was started with a constant nominal supply voltage of *400 V* and a linear load coefficient $B_L = 0.0120$.

Analytical expressions based on Thevenin's theorem and Kloss's equation were compared with the experimental results to validate the accuracy of the models. Initially, the experimental IM slightly oscillates, but it follows the characteristics of the Thevenin model very well. In the steady state, the experimental results agree well with the analytical expressions, confirming the precision of the theoretical models. This agreement indicates that the analytical models successfully predict the behaviour of the IM under linear loading, providing reliable data for further analysis and application.

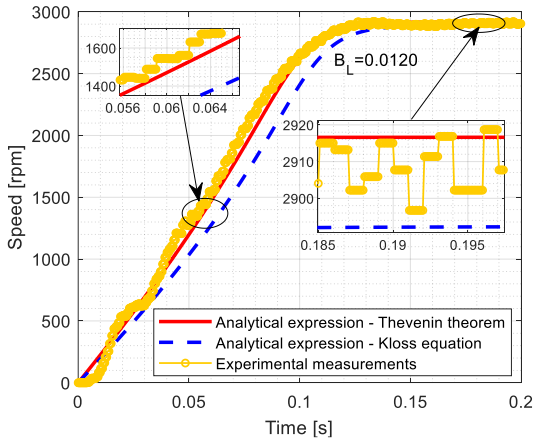

Fig. 9. Experimental results of the speed-time characteristics of the IM under linear loading.

C. Fan Load Type

Figure 10 shows the results of the experimental validation of the analytical expressions for the speed-time characteristics of a IM started directly. IM started with a fan load coefficient $B_F = 0.00003914$ and a constant voltage of *400 V*. In the initial time period of *0.07 s*, the Thevenin model closely followed the experimental results, while the Kloss model showed a slight deviation. In the steady state, where the rotational speed of the IM is approximately *2900 rpm*, there is a very good alignment between the theoretical expressions and the experimental results. This confirms that analytical models can accurately predict the behaviour of the machine not only during transient periods but also in the steady state.

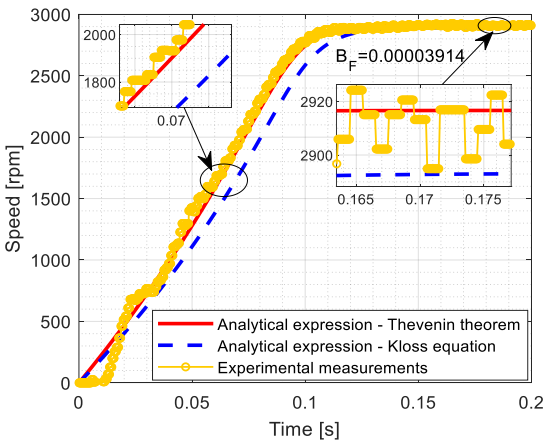

Fig. 10. Experimental results of the speed-time characteristics of the IM under fan loading.

D. Gravitational Load Type

Figure 11 presents the results of the validation of analytical expressions with experimental measurements under a gravitational (constant) load. The IM was loaded with a gravitational load coefficient of $B_G = 1.456$ and powered by a constant voltage of *400 V*. The results show a very good match between the analytical expressions for the start-up time of the IM under constant load and the experimental measurements under the same conditions. The analytical expressions closely follow the experimental measurements throughout the entire start-up process. In steady-state, the match can be considered almost ideal, confirming the validity of theoretical models for describing the machine dynamics under gravitational load.

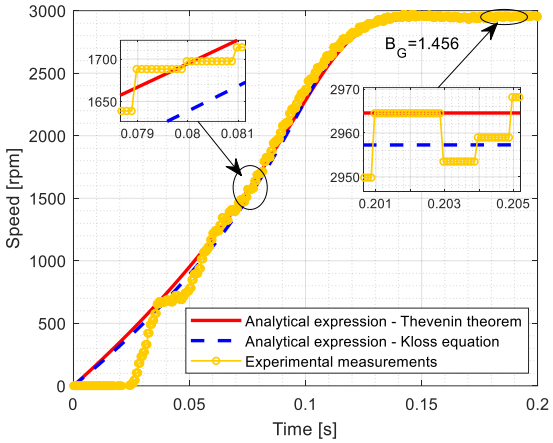

Fig. 11. Experimental results of the speed-time characteristics of the IM under gravitational loading.

E. Performance of Shipboard Loads at the Same Operating Point

To analyse the performance of different loads, experimental measurements of speed-time characteristics were conducted at the same operating point. Figure 12 shows the torque-speed graph of the experimental machine, which illustrates the operating point where the start-up analysis of the IM was performed under different shipboard loads. The experimental measurements were conducted with a fan load coefficient of $B_F = 0.000015183$, a linear load coefficient of $B_L = 0.0047$, and a gravitational load coefficient of $B_G = 1.456$, with a constant supply voltage of *400 V*.

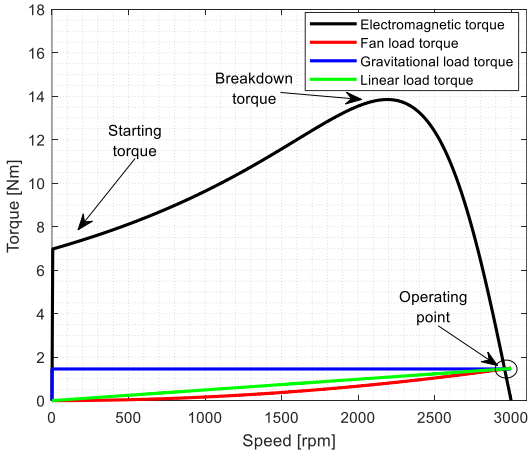

Fig. 12. Torque-speed characteristics of the experimental IM with the operating point where comparisons were made.

Figure 13 shows the speed-time characteristics of a directly started IM to compare the start-up times for different loads at

the same operating point. Figure 13(a) presents the results obtained through analytical expressions derived from Thevenin's expression for torque obtained from the equivalent circuit of Thevenin, while Fig. 13(b) shows the results obtained from experimental measurements at the same operating point. The results indicate that the shortest start-up time is required for the fan load, followed by the linear load, while the gravitational load requires the longest time to reach the steady state.

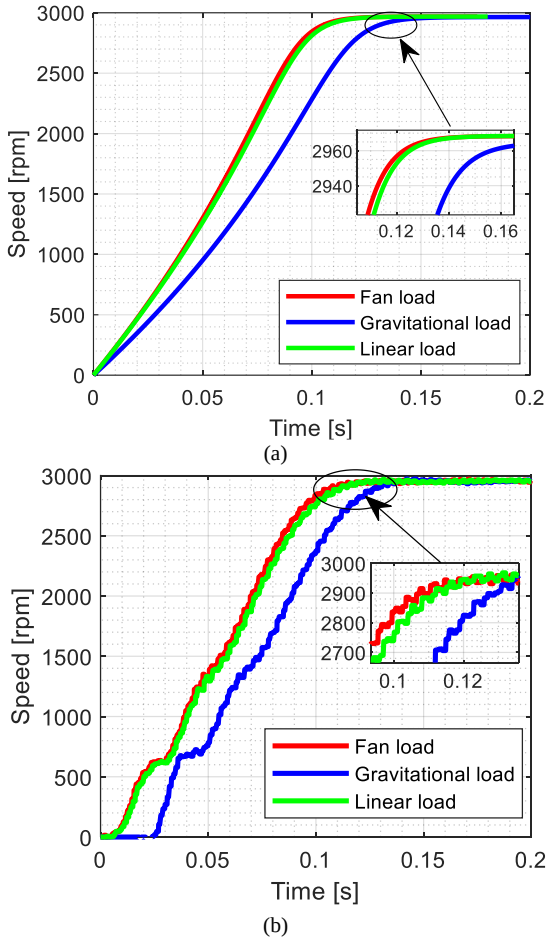

Fig. 13. Speed-time characteristics at the same operating point and under no-load conditions: (a) Results obtained through the Thevenin model; (b) Results obtained from experimental measurements.

V. CONCLUSIONS

This paper reviewed and validated analytical expressions for the IM start-up time under various shipboard operating conditions. The speed-time characteristics obtained from both simulations and experimental measurements closely matched analytical predictions, particularly those based on the Thevenin theorem, while the Kloss torque formula showed slight deviations as it is an approximation derived from the Thevenin model.

The results indicate that the IM reached a steady state fastest when there was no load. Among the different types of loads, the fan load allowed the machine to reach steady state in the shortest time. Specifically, for the fan load, the duration of the start process was about *0.13* seconds. However, with other types of loads, the starting process time is longer. For the observed experimental machine, the starting process took *0.14* seconds under linear load and *0.16* seconds under gravitational load. The time period for reaching a steady state under fan loading was approximately *8 %* shorter compared to linear load, and *19 %* shorter compared to gravitational load.

CONFLICTS OF INTEREST

The authors declare that they have no conflicts of interest.

REFERENCES

[1] M. R. Patel, *Shipboard Electrical Power Systems*, 2nd ed., CRC Press, 2021. DOI: 10.1201/9781003191513.

[2] A. Vagati, A. Fratta, G. Franceschini, and P. Rosso, "AC motors for high-performance drives: A design-based comparison", *IEEE Transactions on Industry Applications*, vol. 32, no. 5, pp. 1211–1219, 1996. DOI: 10.1109/28.536885.

[3] F. Wang, Z. Zhang, T. Ericsen, R. Raju, R. Burgos, and D. Boroyevich, "Advances in power conversion and drives for shipboard systems", *Proceedings of the IEEE*, vol. 103, no. 12, pp. 2285–2311, 2015. DOI: 10.1109/JPROC.2015.2495331.

[4] D. T. Hall, *Practical Marine Electrical Knowledge*, 2nd ed., Witherby, 1999.

[5] J. Yu *et al*, "Identifying the Causes of Ship Collisions Accident Using Text Mining and Bayesian Networks", Elektronika ir Elektrotechnika, vol. 29, no. 6, pp. 58-67, 2023. DOI: 10.5755/j02.eie.35630.

[6] A. F. Molland (Ed.), *The Maritime Engineering Reference Book: A Guide to Ship Design, Construction and Operation*. Oxford: Butterworth-Heinemann, 2008, pp. 344–482. DOI: 10.1016/B978-0-7506-8987-8.00006-8.

[7] J. L. Kirtley, A. Banerjee, and S. Englebretson, "Motors for ship propulsion", *Proceedings of the IEEE*, vol. 103, no. 12, pp. 2320–2332, 2015. DOI: 10.1109/JPROC.2015.2487044.

[8] L. Mrdovic, N. Pudar, I. Knezevic, M. Calasan, S. Cvrk, and T. Dlabac, "Improvement of education in the field of marine engineering at the Faculty of Maritime Studies Kotor", in *Proc. of 2023 10th International Conference on Electrical, Electronic and Computing Engineering (IcETRAN)*, 2023, pp. 1–6. DOI: 10.1109/IcETRAN59631.2023.10192127.

[9] J. M. Prousalidis, P. Mouzakis, E. Sofras, D. Muthumuni, and O. Nayak, "On studying the power supply quality problems due to thruster start-ups", in *Proc. of 2009 IEEE Electric Ship Technologies Symposium*, 2009, pp. 440–448. DOI: 10.1109/ESTS.2009.4906549.

[10] M. Konuhova, "Modeling of induction motor direct starting with and without considering current displacement in slot", *Applied Sciences*, vol. 14, no. 20, p. 9230, 2024. DOI: 10.3390/app14209230.

[11] M. Abbas, M. A. Majeed, M. Kassas, and F. Ahmad, "Motor starting study for a urea manufacturing plant", in *Proc. of 2011 International Conference on Power Engineering, Energy and Electrical Drives*, 2011, pp. 1–6. DOI: 10.1109/PowerEng.2011.6036562.

[12] W. A. Silva *et al.*, "Generalized predictive control robust for position control of induction motor using field-oriented control", *Electrical Engineering*, vol. 97, no. 3, pp. 195–204, 2015. DOI: 10.1007/s00202-014-0326-x.

[13] A. B. Ozer and E. Akin, "Chaos control in vector-controlled induction motor drive", *Electric Power Components and Systems*, vol. 36, no. 7, pp. 733–740, 2008. DOI: 10.1080/15325000701881977.

[14] P. Gnaciński *et al.*, "Power quality and energy-efficient operation of marine induction motors", *IEEE Access*, vol. 8, pp. 152193–152203, 2020. DOI: 10.1109/ACCESS.2020.3017133.

[15] D. Kumar and F. Zare, "A comprehensive review of maritime microgrids: System architectures, energy efficiency, power quality, and regulations", *IEEE Access*, vol. 7, pp. 67249–67277, 2019. DOI: 10.1109/ACCESS.2019.2917082.

[16] J. Barros and R. I. Diego, "A review of measurement and analysis of electric power quality on shipboard power system networks", *Renewable and Sustainable Energy Reviews*, vol. 62, pp. 665–672, 2016. DOI: 10.1016/j.rser.2016.05.043.

[17] I. K. Pallis, I. P. Georgakopoulos, and E. C. Tatakis, "Modern starting methods of large thrusters supplied by the power network of a ship", in *Proc. of 2014 International Conference on Electrical Machines (ICEM)*, 2014, pp. 2325–2331. DOI: 10.1109/ICELMACH.2014.6960510.

[18] L. Maharjan, S. Wang, and B. Fahimi, "Structural analysis of induction machine and switched reluctance machine", *Electric Power Components and Systems*, vol. 47, nos. 1–2, pp. 164–180, 2019. DOI: 10.1080/15325008.2019.1575934.

[19] A. Hughes, *Electric Motors and Drives: Fundamentals, Types and Applications*, 3rd ed., Newnes, 2006.

[20] M. A. Badr, M. A. Abdel-Halim, and A. I. Alolah, "A nonconventional method for fast starting of three phase wound-rotor induction motors", *IEEE Transactions on Energy Conversion*, vol. 11, no. 4, pp. 701–707, 1996. DOI: 10.1109/60.556366.

[21] S. Kucuk and A. Ajder, "Analytical voltage drop calculations during direct on line motor starting: Solutions for industrial plants", *Ain Shams Engineering Journal*, vol. 13, no. 4, art. 101671, 2022. DOI: 10.1016/j.asej.2021.101671.

[22] A. Banerjee, A. Banerjee, D. P. Saikat Rana, and K. N. Shubhanga, "A study of starting methods for an induction motor using an arbitrary waveform generator", in *Proc. of 2015 International Conference on Advances in Electrical Engineering (ICAEE)*, 2015, pp. 34–37. DOI: 10.1109/ICAEE.2015.7506790.

[23] D. Sarkar and N. K. Bhattacharya, "Approximate analysis of transient heat conduction in an induction motor during star-delta starting", in *Proc. of 2006 IEEE International Conference on Industrial Technology*, 2006, pp. 1601–1606. DOI: 10.1109/ICIT.2006.372592.

[24] J. A. Kay, R. H. Paes, J. G. Seggewiss, and R. G. Ellis, "Methods for the control of large medium-voltage motors; Application considerations and guidelines", in *Proc. of Industry Applications Society 46th Annual Petroleum and Chemical Technical Conference (Cat. No. 99CH37000)*, 1999, pp. 345–353, 1999. DOI: 10.1109/PCICON.1999.806453.

[25] W.-X. Li, J.-G. Lu, M.-S. Liu, and J. Zhao, "Design of intelligent soft-start controller for induction motor", in *Proc. of 2004 International Conference on Machine Learning and Cybernetics (IEEE Cat. No. 04EX826)*, 2004, pp. 908–912, vol. 2. DOI: 10.1109/ICMLC.2004.1382315.

[26] Z. M. Zhao, S. Meng, C. C. Chan, and E. W. C. Lo, "A novel induction machine design suitable for inverter-driven variable speed systems", *IEEE Transactions on Energy Conversion*, vol. 15, no. 4, pp. 413–420, 2000. DOI: 10.1109/60.900502.

[27] P. T. Lagonotte, H. Al Miah, and M. Poloujadoff, "Modelling and identification of parameters of saturated induction machine operating under motor and generator conditions", *Electric Machines & Power Systems*, vol. 27, no. 2, pp. 107–121, 1999. DOI: 10.1080/073135699269334.

[28] H. Benbouhenni, N. Bizon, I. Colak, M. Iliescu, and P. Thounthong, "A new direct torque control of an efficient and cost-effective traction system using two squirrel cage induction motors feed by a single inverter", *Electric Power Components and Systems*, vol. 0, no. 0, pp. 1–21, 2024. DOI: 10.1080/15325008.2024.2325541.

[29] P. Aree, "Precise analytical formula for starting time calculation of medium- and high-voltage induction motors under conventional starter methods", *Electrical Engineering*, vol. 100, no. 2, pp. 1195–1203, 2018. DOI: 10.1007/s00202-017-0575-6.

[30] M. P. Ćalasan, "Analytical solution for no-load induction machine speed calculation during direct start-up", *International Transactions on Electrical Energy Systems*, vol. 29, p. e2777, 2019. DOI: 10.1002/etep.2777.

[31] M. P. Ćalasan, "An invertible dependence of the speed and time of the induction machine during no-load direct start-up", *Automatika*, vol. 61, no. 1, pp. 141–149, 2020. DOI: 10.1080/00051144.2019.1689725.

[32] M. Ćalasan, M. Alqarni, M. Rosić, N. Koljčević, B. Alamri, and S. H. E. Abdel Aleem, "A novel exact analytical solution based on Kloss equation towards accurate speed-time characteristics modeling of induction machines during no-load direct startups", *Applied Sciences*, vol. 11, no. 11, pp. 5102, 2021. DOI: 10.3390/app11115102.

[33] I. Knežević, M. Calasan, and T. Dlabač, "Novel analytical approaches for induction machine direct start-up speed-time curve modeling under fan load", *Electrical Engineering*, vol. 106, pp. 1925–1938, 2023. DOI: 10.1007/s00202-023-02039-3.

[34] I. Knežević, T. Dlabač, M. Ćalasan, and M. Krčum, "Novel approaches to representing the speed-time characteristics of a direct start-up induction machine driving gravitational-type loads", *Brodogradnja*, vol. 75, no. 4, 2024. DOI: 10.21278/brod75402.